Research on Calculation Method of Strength of Packaging Load-carrying Frame

IOP Conf. Series: Materials Science and Engineering **493** (2019) 012004 doi:10.1088/1757-899X/493/1/012004

Research on Calculation Method of Strength of Packaging Load-carrying Frame

Lili Zhang [1, 2, *], Xing Huang [3], Yuan Zhao [1, 2] and Lin Tao [1, 2]

[1]Liaoning Key Laboratory of Information Physics Fusion and Intelligent Manufacturing for CNC Machine, Fushun, China
[2]Shenyang Institute of Technology, Fushun, China
[3]AECC SHENYANG LIMING Aero Engine Co., LTD, Shenyang, China

*Corresponding author e-mail: 94213031@qq.com

Abstract. The load-carrying structure of the engine package has a form of frame. The traditional 3D solid finite element method can be used for strength analysis. The beam element method can also be used for calculation and analysis according to its structural characteristics. The two methods are used to calculate and compare, the advantages and disadvantages of the two methods are analysed, and some suggestions on the application of beam element method are put forward.

1. Introduction

The engine package protects the engine during the storage and transportation of the aeroplane engine. Therefore, its own strength should be guaranteed. It is necessary to ensure its strength meets the requirements through calculation and test in the stage of design. The load-carrying structure of the package has the form of frame. The traditional 3D solid finite element method can be used for finite element strength analysis. The beam element method can also be used for calculation and analysis according to its structural characteristics.

The general beam element is based on the assumption of flat section deformation in elementary mechanics. In this assumption, the bending deformation is considered to be the main deformation, and the shear deformation is a minor deformation and thus can be ignored. In general, the choice of the type and quantity of units depends firstly on the evaluation to the model and the effect, and secondly on the affordable cost and accuracy. In practical engineering, one-dimensional elements are generally used for modeling slender structures. However, the ratio of the directional dimension L to the maximum dimension a of the other two directions can be considered by one-dimensional rods. There is no accepted criterion. One kind of reference is that: when L/d>5, it can be considered a beam. In the engineering structure, the rigid frame is generally simulated by the beam element; the truss is generally simulated by the rod element, such as for the calculation of the secondary stress, the beam element can also be used.

2. Model parameters and calculation status

2.1. Geometric data

The geometric data is based on the overall structural room design drawing. The solid model of the package and the beam model (hereinafter referred to as the two models) are shown in Figure 1-2. The origin of the coordinate system is on the the connecting surface of upper and lower mounting edge, and the Z axis is package length direction, X axis is horizontal direction, Y axis is vertical direction.

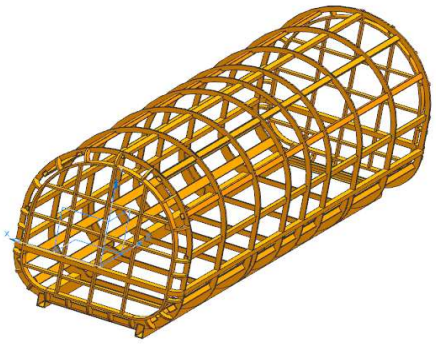

Figure 1. Package solid model diagram

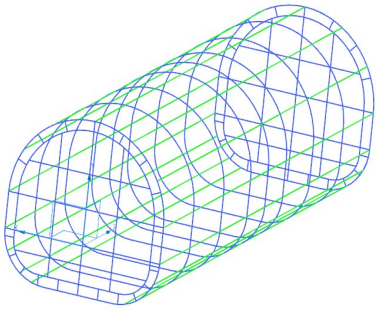

Figure 2. Package beam model

2.2. Material data

The package material is No. 20 steel, density ρ=7850kg/m^3, elastic modulus E=211GPa, Poisson's ratio μ=0.286.

2.3. Calculation state selection

Test status: The package is placed on the ground statically and is subjected to internal gas pressure and package box gravity.

Packing status: The package is placed on the ground statically and is subjected to the gravity of the package and the engine.

Nitrogen seal status: The package is placed on the ground statically and is subjected to internal gas pressure, and the gravity of the package and the engine.

Lifting status: The package is lifted off the ground and is subjected to the gravity of the package and the engine.

3. Finite element model and boundary conditions

3.1. Finite element model and oundary condition application results

The solid model meshing uses solid95 units, which divides 241,371 units and 627,745 nodes. The beam model meshing uses beam188 units, which divides 3601 units and 6780 nodes. The finite element models of the two models are shown in Figure 3-4.

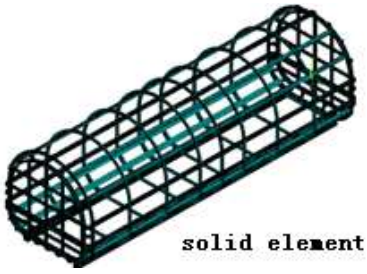

Figure 3. Finite element model diagram of the solid element of the package

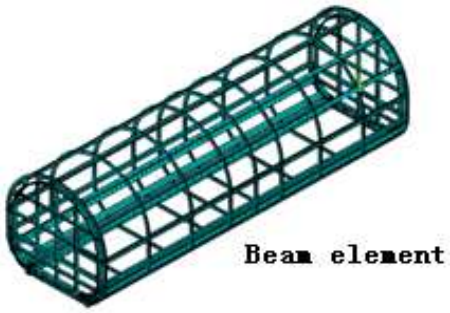

Figure 4. Finite element model diagram of the beam element of the package

3.2. Load

Package gravity load: Y-direction acceleration 9.8 m/s^2

Engine gravity load: The mass of the engine and its bracket is 2200 kg. The gravity is transmitted to the package box through the eight bottom plates under the bracket. The bottom plate of the bracket is at an angle of 45 degrees to the horizontal plane. In the solid unit model, 448 nodes are selected at the corresponding position of the bottom plate to be applied with gravity load, thus through the balance of the force system, it can be shown that the horizontal and vertical forces on each node are:

$$\mathrm{F} = \frac{2200\times9.8}{448}\ \mathrm{N} = 48.125\ \mathrm{N} \tag{1}$$

The beam element model selects 16 key points at the corresponding position of the bottom plate to apply gravity load. Therefore, through the balance of the force system, it can be shown that the horizontal and vertical forces on each node are:

$$\mathrm{F} = \frac{2200\times9.8}{16}\ \mathrm{N} = 1347.5\ \mathrm{N} \tag{2}$$

Gas pressure load: The structure of the package is steel skeleton with a FRP skin. For the solid element model, the total internal gas pressure can be equivalent to the area conversion pressure to be applied to the internal surface of the steel frame. The gas pressure difference between the inside and outside of the package is 52000 Pa, the direction is from the inside of the package to the outside, the total surface area of the skin of the package is 31.51294 m^2, and the surface area of the steel skeleton is 4.11769 m^2. The pressure can be converted:

$$\mathrm{P} = \frac{52000\times31.51294}{4.11769}\ \mathrm{Pa} = 397959\ \mathrm{Pa} \tag{3}$$

The four long beams in the lower part of the package have direct contact with the gas inside the box, and the gas pressure is 52000 Pa.

For the beam element model, the internal gas total pressure can be equivalent to the pressure converted by the beam length to be applied to the beam. The gas pressure difference between the inside and outside of the package is 52000 Pa, the direction is from the inside of the package to the outside, the total surface area of the skin of the package is 31.512941 m^2, and the length of the steel frame under the skin is 103.3824964 m, so the force per unit length can be converted as:

$$\mathrm{F}^* = \frac{52000\times31.51294}{103.3824964}\mathrm{N/m} = 15851\mathrm{N/m} \tag{4}$$

The four long beams in the lower part of the package have an area of 1.9044 m^2 and a length of 21.16 m. The gas pressure subjected is:

$$F^* = \frac{52000 \times 1.9044}{21.16}\ \mathrm{N/m} = 4680\ \mathrm{N/m} \tag{5}$$

The specific application position of the load is shown in Figure 5-6.

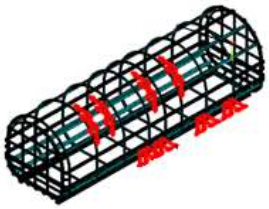

Figure 5. Packing and engine gravity load application diagram

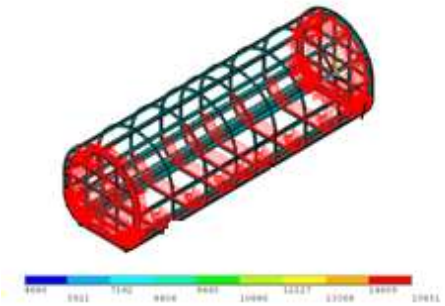

Figure 6. Gas pressure load application diagram

4. Calculation results

In addition to caring about the overall stress distribution results of the package, the upper and lower arch beams of the package were selected as the key assessment sites.

4.1. Test status calculation results

4.1.1. Package deformation results. The overall deformation results of the two models in the test status are shown in Figure 7-8.

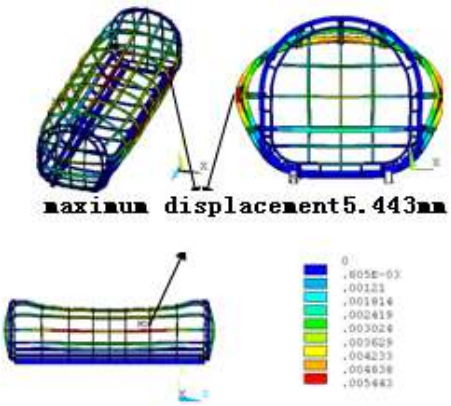

Figure 7. Overall deformation diagram of the test status solid model

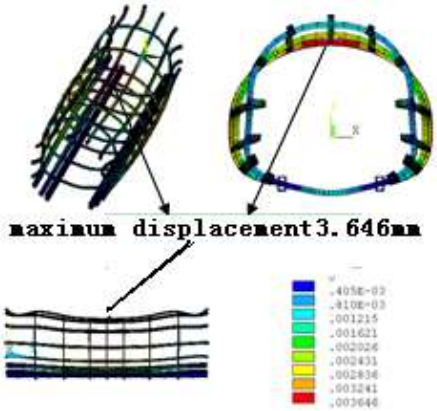

Figure 8. Overall deformation diagram of the test status beam model

4.1.2. Package stress results. The stress distribution results of the two models in the test status are shown in Figure 9-12.

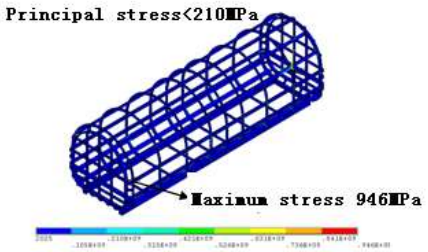

Figure 9. Overall stress cloud diagram of solid model in the test status

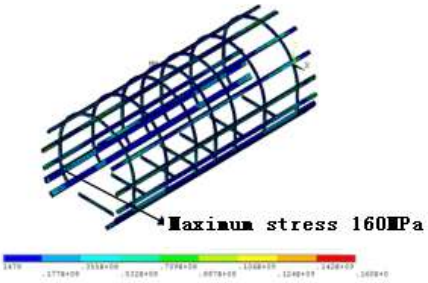

Figure 10. Overall stress cloud diagram of beam model in the test status

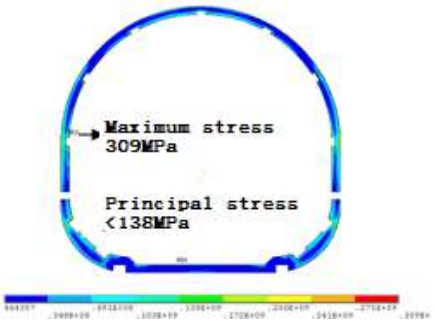

Figure 11. Stress cloud diagram of the arch beam solid model in the test status

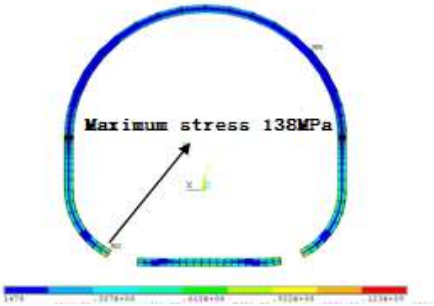

Figure 12. Stress cloud diagram of the beam model in the test status

4.2. Package status calculation results

4.2.1. Package deformation results. The overall deformation results of the two models in the package status are shown in Figure 13-14.

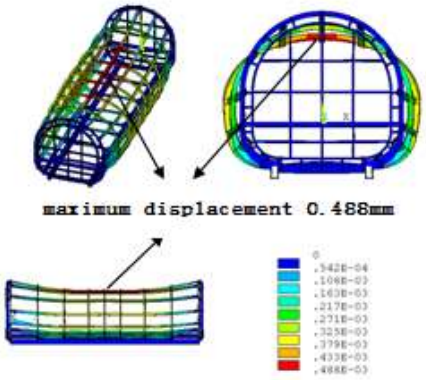

Figure 13. Overall deformation of solid model in the package status

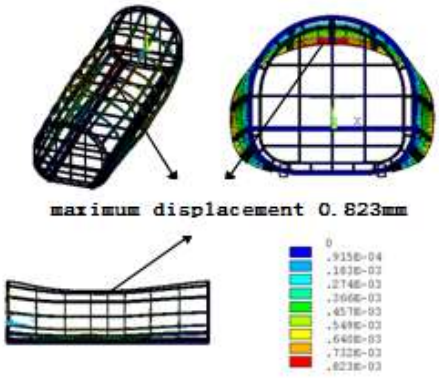

Figure 14. Overall deformation of the beam model in the package status

4.2.2. Package stress results. The overall stress distribution results of the two models in the package status are shown in Figure 15-18.

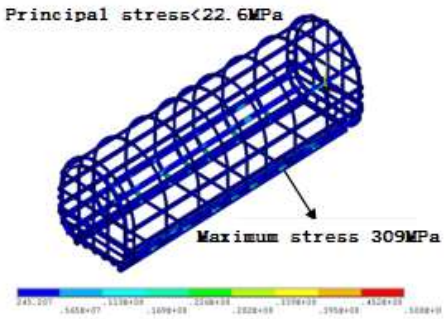

Figure 15. Overall stress cloud diagram of the solid model in package status

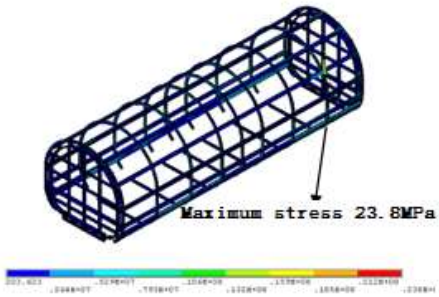

Figure 16. Overall stress cloud diagram of the beam model in package status

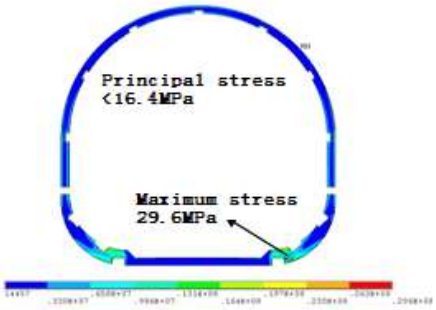

Figure 17. tress cloud diagram of the arch beam solid model in package status

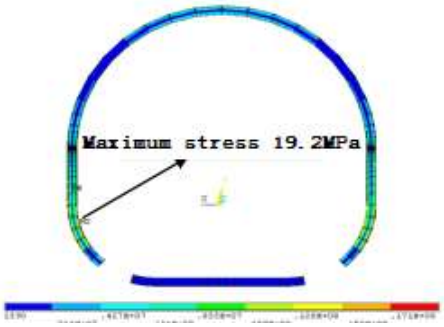

Figure 18. Stress cloud diagram of the arch beam beam model in package status

4.3. Nitrogen seal status calculation results

4.3.1. Package deformation results. The overall deformation results of the two models in the nitrogen seal status are shown in Figure 19-20.

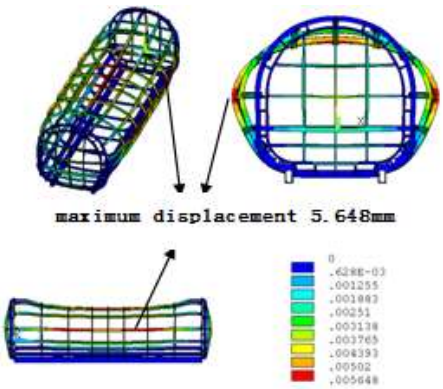

Figure 19. Overall deformation of solid model in the nitrogen seal status

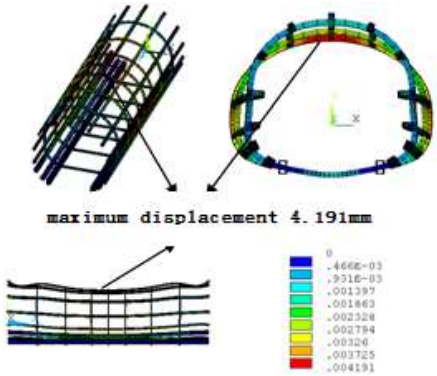

Figure 20. Overall deformation diagram of the beam model in nitrogen seal status

4.3.2. Package stress results. The stress distribution results of the two models in the nitrogen seal status are shown in Figure 21-24.

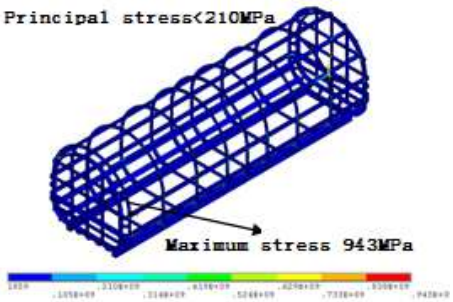

Figure 21. Overall stress cloud diagram of the solid model in nitrogen seal status

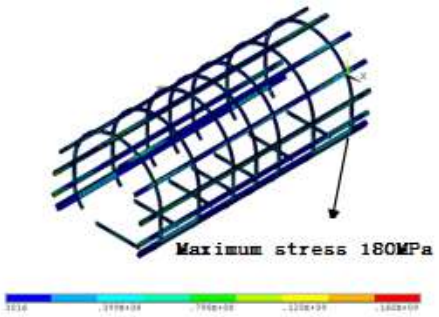

Figure 22. Overall stress cloud diagram of the beam model in nitrogen seal status

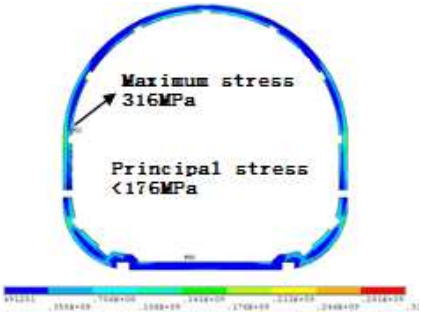

Figure 23. Stress cloud diagram of the arch beam solid model in nitrogen seal status

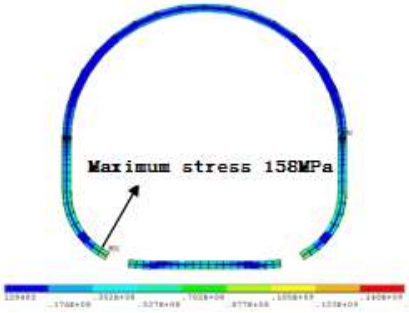

Figure 24. Stress cloud diagram of the arch beam beam model in nitrogen seal status

4.4. Lifting status calculation process and results

4.4.1. Package deformation results. The overall deformation results of the two models in the lifting status are shown in Figure 25-26.

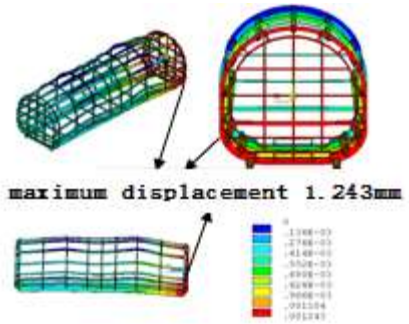

Figure 25. Overall deformation diagram of the solid model in lifting status

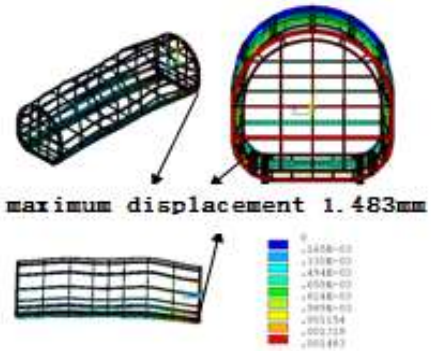

Figure 26. Overall deformation diagram of the beam model in lifting status

4.4.2. Package stress results. The stress distribution results of the two models in the lifting status are shown in Figure 27-30.

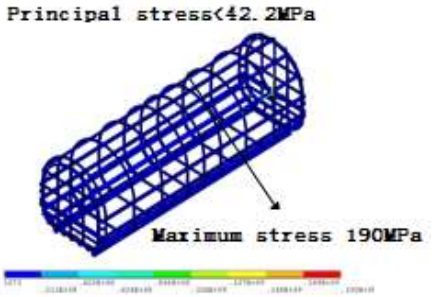

Figure 27. Overall stress cloud diagram of the solid model in lifting status

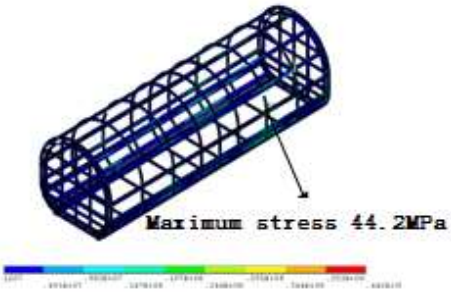

Figure 28. Overall stress cloud diagram of the beam model in lifting status

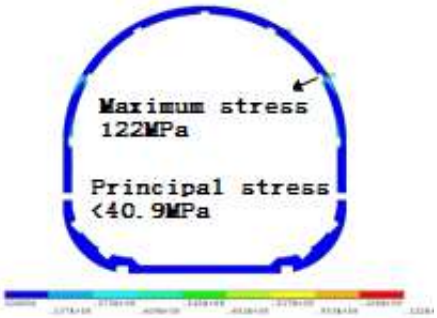

Figure 29. Arch beam stress cloud diagram of the solid model in lifting status

Figure 30. Arch beam stress cloud diagram of the beam model in lifting status

5. Results comparison and analysis

The calculation results of the solid model are shown in Table 1-2.

Table 1. Maximum displacement table of the solid model in each calculation status

Calculation status	Test status	Package status	Nitrogen seal status	Lifting status
Maximum displacement value (mm)	5.443	0.488	5.648	1.243

Table 2. Maximum stress table of the solid model in each calculation status

Calculation status	Test status	Package status	Nitrogen seal status	Lifting status
Overall maximum stress value (MPa)	946	50.8	943	190
Maximum stress value of arch beam(MPa)	309	29.6	316	122

The calculation results of the beam model are shown in Table 3-4.

Table 3. Maximum displacement table of the beam model in each calculation status

Calculation status	Test status	Package status	Nitrogen seal status	Lifting status
Maximum displacement value (mm)	3.646	0.823	4.191	1.483

Table 4. Maximum stress table of the beam model in each calculation status

Calculation status	Test status	Package status	Nitrogen seal status	Lifting status
Overall maximum stress value (MPa)	160	23.8	180	44.2
Maximum stress value of arch beam(MPa)	138	19.2	158	44.2

The stress comparison of the stress between the beam model and the main parts of the solid model is shown in Table 5.

Table 5. Maximum stress table of the beam model and the main parts of the solid model in each calculation status

Inspection site	Model type	Maximum stress value (MPa)			
		Test	Package	Nitrogen seal	Lifting
Overall	Beam model	160	23.8	180	44.2
	The main part of the solid model	<210	<22.6	<210	<42.2
Arch beam	Beam model	138	19.2	158	44.2
	The main part of the solid model	<138	<16.4	<176	<40.9

It can be seen from the above table that the stress calculation result of the beam model is close to the stress level of the main part of the solid model, which can be used to describe the stress distribution of the main part of the package; the maximum stress value of the solid model reflects the stress concentration of the dangerous part of the package. Effective measures should be taken to ensure the safety of dangerous parts.

6. Improvement measures for beam unit calculation method

The beam element calculation method has the advantages of uniform mesh division, low computer computing ability requirements, clear calculation results which is easy for analysis, and it is proved by this calculation that it is suitable for strength analysis of such package structures. However, in the specific calculation process, it is found that the beam element calculation method should be improved in the following aspects:

a. For the modeling aspect, attentions should be paid to the spatial geometric characteristics of the structure, and the stress of the plugs at the front and back of the package and the arc structure at the junction of the package should be faithful to the actual structure. This calculation model is simplified at these positions, resulting in distortion of the calculation results of the front and rear plugs, and may have an adverse effect on the package part.

b. The mesh of the contact parts between the beams should be more matched to avoid excessive changes in the mesh density.

c. The stress results that constrains the applied site has distortion. The constrained loading should be optimized or measures should be taken during the modeling phase to eliminate this effect.

d. The replacement calculation and application of the gas pressure load are to be further optimized.

Acknowledgments

This work was financially supported by national Natural Science Foundation Youth Fund(61603262) and research Fund of i5 Institute of Shenyang Institute of Technology(i5201701) fund.

References

[1] A new mathematical model for determining the longitudinal strain in cold roll forming process. Liu Chengfang,et al.The International Journal of Advanced Manufacturing Technology . 2015

[2] Electro-thermal modeling and experimental validation for lithium ion battery[J] . Yonghuang Ye,Yixiang Shi,Ningsheng Cai,Jianjun Lee,Xiangming He. Journal of Power Sources . 2011

[3] Performance Assessment of an Allothermal Auger Gasification System for On-Farm Grain Drying[J] Samy Sadaka,Mahmoud Sharara,Gagandeep Ubhi. Journal of Sustainable Bioenergy Systems . 2014 (01)

[4] Force analysis of clogging arches in a silo. R.C.Hidalgo,C.Lozano,I.Zuriguel,A.Garcimartin. Granular Matter . 2013

[5] Thermal analysis of a ceramic coating diesel engine piston using 3-D finite element method[J] . Ekrem Buyukkaya,Muhammet Cerit. Surface & Coatings Technology . 2007 (2)